

Effect of spatial hole burning on a dual-wavelength mode-locked laser based on compactly combined dual gain media

Y. J. Huang,¹ Y. S. Tzeng,¹ H. H. Cho,¹ and Y. F. Chen^{1,2,*}

¹Department of Electrophysics, National Chiao Tung University, Hsinchu 30010, Taiwan

²Department of Electronics Engineering, National Chiao Tung University, Hsinchu 30010, Taiwan

*Corresponding author: yfchen@cc.nctu.edu.tw

Received July 4, 2014; revised September 9, 2014; accepted September 10, 2014;
posted September 15, 2014 (Doc. ID 216393); published October 16, 2014

The effect of spatial hole burning (SHB) on dual-wavelength self-mode-locked lasers based on physically combined Nd:YVO₄/Nd:LuVO₄ and Nd:YVO₄/Nd:KGW composite active medium is comparatively investigated. The length of the first Nd:YVO₄ crystal is optimized to realize a highly compact and efficient TEM₀₀-mode picosecond laser at 1.06 μm with optical conversion efficiency greater than 20%. When the SHB effect is enhanced by decreasing the separation between the input end mirror and the composite gain medium, it is experimentally found that not only the pulse duration monotonically decreases, but also the temporal behavior gradually displays a narrow-peak-on-a-pedestal shape for the Nd:YVO₄/Nd:LuVO₄ scheme, while the multipulse operation can be obtained for the Nd:YVO₄/Nd:KGW configuration. These phenomena are further explored by numerically simulating mode-locked pulses from the experimentally measured optical spectra. © 2014 Chinese Laser Press

OCIS codes: (140.3480) Lasers, diode-pumped; (140.3530) Lasers, neodymium; (140.3580) Lasers, solid-state; (140.4050) Mode-locked lasers.

<http://dx.doi.org/10.1364/PRJ.2.000161>

1. INTRODUCTION

Dual-wavelength light sources are useful for a variety of scientific research and applied studies [1]. To achieve stable dual-wavelength operation in solid-state lasers, the gain competition between each spectral line should be avoided as much as possible. By deliberately designing the laser cavity, the aforementioned problem can be appropriately solved. However, this usually causes the whole resonator to be relatively bulky and complex [2–5]. With great progress in the growth of optical materials, a series of disordered crystals, generally characterized by multiple fluorescent peaks with comparable spectral intensities, has been successfully realized to be inherently desirable for dual-wavelength emission [6–11]. Because of the easy implementation, directly using the disordered crystals as the active media is by far the most popular way to obtain dual-wavelength ultrashort lasers around 1 μm with the passively mode-locked technique [8–11]. However, the uncontrollable intensities between each emission component present the main challenge for such lasers to be used in various practical applications.

To date, using a semiconductor saturable absorber mirror (SESAM) to lock the phases of all longitudinal modes is the most powerful technique for passive mode locking with a repetition rate in the several hundred megahertz range [12,13]. However, to push the repetition rate into the gigahertz region, the SESAM must be carefully designed to have a very small modulation depth (below 1%) for satisfying the *Q*-switching instability criterion [14–16]. This indicates that such small modulation depth may be offered by the nonlinearity of the gain medium itself. We recently observed that by shortening the cavity length to reduce the number of longitudinal modes,

a quite stable self-mode-locking in solid-state lasers could be achieved with a repetition rate of up to several gigahertz, and this interesting phenomenon has been widely observed in various laser systems [17–21]. More recently, we originally proposed a method to achieve a diode-end-pumped dual-wavelength picosecond laser with self-mode-locking [22]. The operational principle relies on the fact that two laser crystals are physically combined as a composite gain medium sharing the same optical resonator for delivering two-color emission with parallel polarizations. Through the optical beating between two carrier frequencies of dual-color synchronous pulses, a stream of terahertz-repetition-rate pulses was further generated. However, the optical conversion efficiency was quite limited due to the insertion of an intracavity aperture for guaranteeing the fundamental transverse mode oscillation.

In this work, we show that the proposed method of physically combining dual gain media can also be applied in Nd:YVO₄ and Nd:LuVO₄ crystals for simultaneous emissions at 1064 and 1065 nm, as well as in Nd:YVO₄ and Nd:KGW crystals for simultaneous emissions at 1064 and 1067 nm. It is theoretically analyzed and experimentally verified that shortening the length of the first Nd:YVO₄ crystal is beneficial to suppress the excitation of high-order transverse modes for achieving reliable dual-wavelength self-mode-locked operation with the TEM₀₀ mode oscillation. As a consequence, the optical conversion efficiency can be significantly improved to be higher than 20% as compared with our previous work. Since the effect of spatial hole burning (SHB) in the gain medium has been recognized to play an important role in mode-locked solid-state lasers [23–26], we further

systematically explore the influence of the SHB effect on the mode-locked performance of our dual-wavelength laser. By decreasing the separation between the input end mirror and the gain medium, it is found that not only the pulse duration will continuously decrease thanks to the enhanced SHB effect, but also that the temporal behavior gradually displays a narrow-peak-on-a-pedestal shape for the Nd:YVO₄/NdLuVO₄ scheme and a multipulse shape for the Nd:YVO₄/Nd:KGW configuration. These phenomena are numerically simulated and well explained by a mathematical model expressed as a sum of all fields of two synchronous mode-locked groups.

2. EXPERIMENTAL SETUP

The experimental configuration for the diode-end-pumped dual-wavelength synchronously self-mode-locked laser is schematically shown in Fig. 1(a). The input end mirror is a plano-concave mirror with a radius of curvature of 1000 mm. It is coated to be antireflective at 808 nm on the plane side, and is coated to be highly transmissive at 808 nm and highly reflective at 1.06 μm on the concave side. The composite active medium consisted of two vanadate laser materials. The first one was a 0.2% *a*-cut Nd:YVO₄ crystal with dimensions of 3 mm \times 3 mm \times 3 mm, and it was closely contacted by a 0.5% *a*-cut Nd:LuVO₄ crystal with dimensions of 3 mm \times 3 mm \times 8 mm. The crystallographic *c* axes for both materials were oriented to be parallel to each other. All end facets of the vanadate materials were coated to be antireflective at the pump and lasing wavelengths. The composite active medium was wrapped with indium foil and mounted in a water-cooled copper holder with a temperature of 16°C. The pump source was a 6 W fiber-coupled laser diode at 808 nm

with a core diameter of 200 μm and a numerical aperture of 0.22. A pair of the plano-convex coupling lenses with focal lengths of 25 mm and total transmission efficiency of 88% was utilized to reimagine the pump beam into the composite active medium with a pump radius of approximately 120 μm . The waist position of the pump beam z_0 , as indicated in Fig. 1(a), could be freely adjusted for acquiring the optimally balanced dual-wavelength intensities. A flat wedged mirror with reflectivity of 95% at 1.06 μm was employed as the output coupler. The geometrical length of laser cavity L_{cav} was set to be around 25 mm. Therefore, the optical cavity length is estimated to be 38.7 mm if taking the refractive indices of the materials into account, corresponding to a free spectral range of 3.88 GHz. The separation d between the input end mirror and the composite active medium was initially fixed to be 6 mm, and it could be adjusted to precisely control the spectral bandwidth via the SHB effect [27]. The laser mode radius was evaluated to be in the range of 180–190 μm .

The real-time temporal behavior of the mode-locked pulses was monitored by a high-speed InGaAs photodetector with rise time of 35 ps, and the received signal was sent to a digital oscilloscope (Agilent, DSO 80000) with electrical bandwidth of 12 GHz and sampling interval of 25 ps. A Fourier optical spectrum analyzer (Advantest, Q8347) that is constructed based on a Michelson interferometer was used to record the spectral information of the laser output with a resolution of 0.003 nm. Since the mode spacing for the free spectral range of 3.88 GHz is equal to 0.015 nm, the longitudinal modes can be clearly resolved. The fine structure of the mode-locked pulses was measured with the help of a commercial autocorrelator (APE pulse check, Angewandte Physik and Elektronik GmbH).

3. PERFORMANCE OF A DUAL-WAVELENGTH PICOSECOND LASER

First of all, we use the analytical expressions derived in [28] on the basis of the space-dependent rate equation analysis to calculate the variations of output powers radiating from Nd:YVO₄ and Nd:LuVO₄ crystals with the following experimental parameters: $\lambda_p = 808 \text{ nm}$, $R_{\text{OC},1} = R_{\text{OC},2} = 0.95$, $L_1 = L_2 = 0.003$, $\omega_1 = 190 \mu\text{m}$, $\omega_2 = 180 \mu\text{m}$, $\omega_{p0} = 120 \mu\text{m}$, $M^2 = 280$, $\alpha_1 = 0.22 \text{ mm}^{-1}$, $\alpha_2 = 0.4 \text{ mm}^{-1}$, $l_{\text{cry},0} = 0 \text{ mm}$, $l_{\text{cry},1} = 3 \text{ mm}$, $l_{\text{cry},2} = 8 \text{ mm}$, $I_{\text{sat},1} = 7.473 \text{ W/mm}^2$, $I_{\text{sat},2} = 11.965 \text{ W/mm}^2$, $n_1 = 2.222$, $n_2 = 2.255$, and $\eta_{Q,1} = \eta_{Q,2} = 1$, with the subscripts 1 and 2 representing the quantities for the Nd:YVO₄ crystal at $\lambda_1 = 1064 \text{ nm}$ and the Nd:LuVO₄ crystal at $\lambda_2 = 1065 \text{ nm}$. The computed result for the incident pump power P_{in} of 4.4 W is depicted in Fig. 1(b) as a function of parameter z_0 . The experimental data are also recorded in Fig. 1(b) and are found to agree well with the theoretical analysis. Just like our previous study with the Nd:YVO₄ and Nd:GdVO₄ crystals, the output power ratio between the 1064 and 1065 nm radiations can be flexibly controlled simply by varying the waist location of the pump beam. More importantly, the required offset D from the maximum output power at 1064 nm to the gain-balanced point, as indicated in Fig. 1(b), is only 1.8 mm, which is considerably smaller than the value of 3.8 mm obtained in [28]. Note that the parameter D stands for the degree of defocusing in the end-pumped configuration; the larger the parameter D , the more high-order transverse modes would probably oscillate, and vice versa. Consequently, the

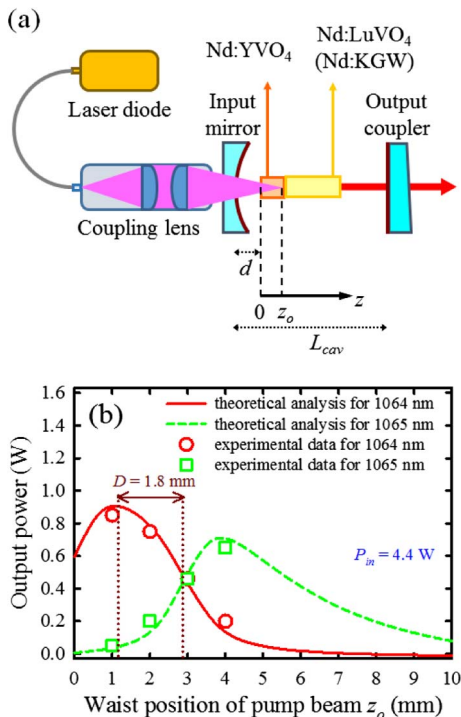


Fig. 1. (a) Experimental configuration for the diode-pumped dual-wavelength mode-locked Nd-doped laser. (b) Theoretical calculations and experimental data of output powers at 1064 and 1065 nm versus the waist position of the pump beam.

present dual-wavelength Nd:YVO₄/Nd:LuVO₄ scheme is potentially feasible in generating the fundamental transverse mode without the need of an intracavity aperture. This is experimentally verified by the oscilloscope traces shown in Figs. 2(a) and 2(b) with time spans of 50 and 2 ns, respectively. It can be seen that a quite stable pulse train without any modulation caused by the beat frequency between transverse modes is implemented. The beam quality factors were also measured to be better than 1.2 in both directions for confirming the TEM₀₀ mode oscillation. Figure 2(c) describes the total output power versus the incident pump power for the developed dual-wavelength laser. At least 95% of the pump power was absorbed by the composite gain medium, and the unabsorbed pump power is separated by a dichroic mirror when measuring the laser output power. Since no intracavity aperture is needed in the present setup, the optical conversion efficiency could be significantly enhanced to reach 20% as compared to the value 10% obtained in our previous studies [22,28]. Under an incident pump power of 4.5 W, this miniature dual-wavelength light source is able to efficiently deliver the total output power of 1 W at 1.06 μm . The great improvement of the optical conversion efficiency manifestly shows the advantage of shortening the length of the first Nd:YVO₄ crystal in our proposed dual-wavelength TEM₀₀-mode laser. By simultaneously considering the lasing thresholds for different high-order transverse modes as a function of the parameter z_0 and our developed dual-wavelength analysis, the length of the first gain material may be theoretically optimized to give the best case for efficient laser output with high-order transverse modes suppressed, which is under investigation.

A typical optical spectrum under gain balancing is depicted in Fig. 3(a) with the peak wavelengths of 1064.38 and 1065.82 nm for each spectral component, whereas the auto-correlation trace of the mode-locked pulses is recorded in Fig. 4(a) with the full width at half-maximum (FWHM) measured to be about 59.4 ps. If we assume the temporal intensity to follow the Gaussian shape, the pulse width could be deduced to be 42 ps. Furthermore, a quasi-periodic fringe, as a result of the temporal interference between two carrier frequencies of dual-color synchronous pulses, is obtained with an optically beat frequency of around 0.37 THz and

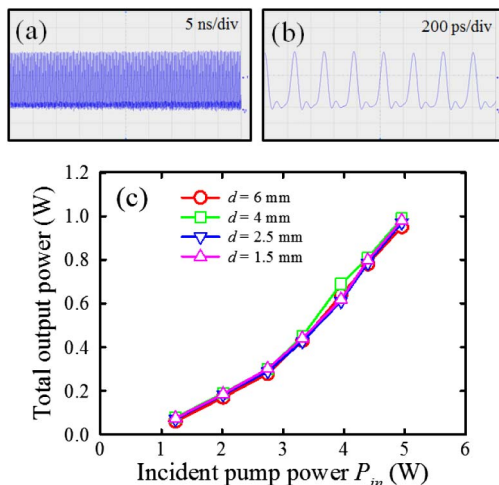


Fig. 2. Oscilloscope traces with time spans of (a) 50 ns and (b) 2 ns. (c) Total output power at 1.06 μm versus the incident pump power for different separations d .

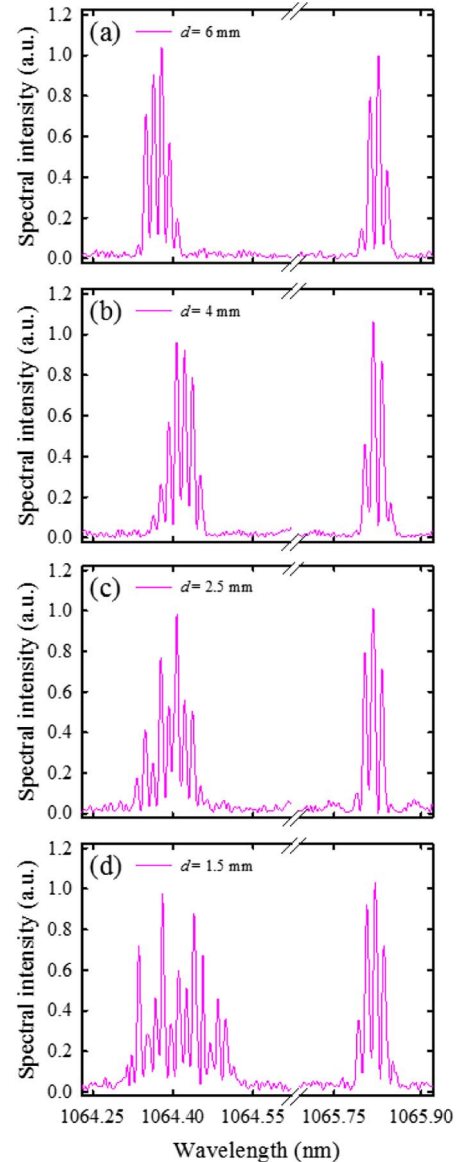


Fig. 3. Optical spectra of picosecond Nd:YVO₄/Nd:LuVO₄ laser for (a) $d = 6$ mm, (b) $d = 4$ mm, (c) $d = 2.5$ mm, and (d) $d = 1.5$ mm.

effective pulse duration of 1.4 ps, as depicted in Fig. 4(e). To individually measure the properties for each spectral line that are very close to each other, perhaps an optical Bragg grating could be employed, just like the chirped fiber Bragg grating is used in a tri-wavelength ultrafast fiber laser [29].

The relatively compact structure of the current setup enables us to readily investigate the influence of the SHB effect on the mode-locked performance of our dual-wavelength laser. For a standing-wave cavity, it is well known that the amount of the SHB effect could be controlled by varying the separation between the input end mirror and the gain medium [23–26]. Thanks to the enhancement of the SHB effect, the pulse width for the case of gain-at-the-end (GE) scheme is found to be shorter than that of gain-in-the-middle (GM) architecture under the same cavity configuration. Motivated by this, we carefully varied the separation between the input end mirror and the gain medium to properly record the corresponding optical spectra. The experimental results are

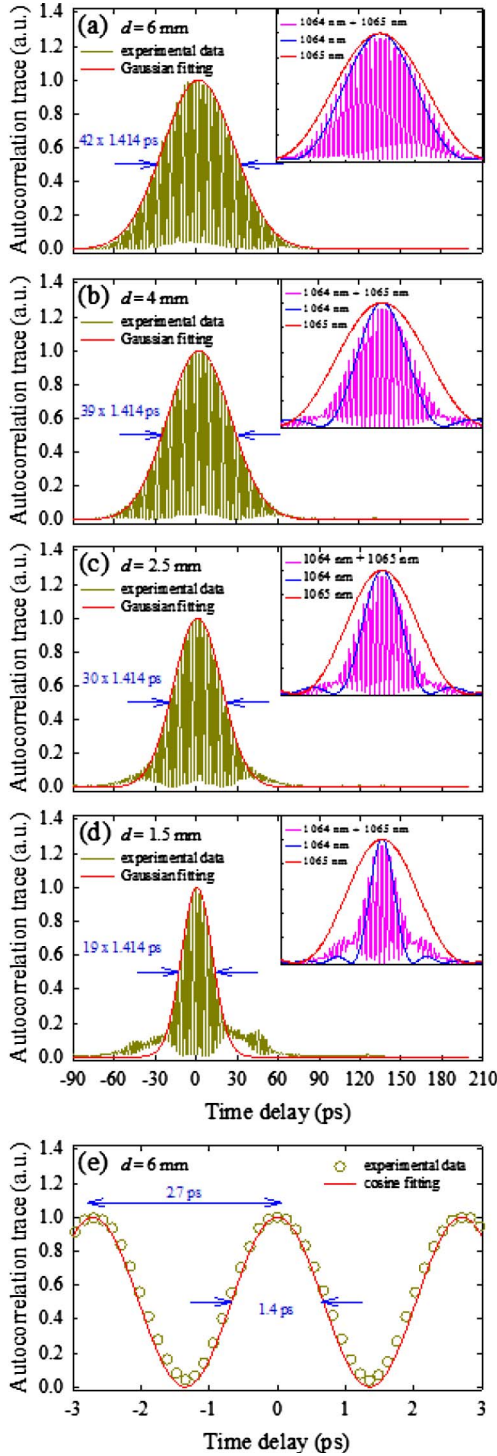


Fig. 4. Experimental autocorrelation traces and numerically reconstructed pulse shapes of a picosecond Nd:YVO₄/Nd:LuVO₄ laser for (a) $d = 6$ mm, (b) $d = 4$ mm, (c) $d = 2.5$ mm, and (d) $d = 1.5$ mm. (e) Detailed structure of the optically beat pulse.

shown in Figs. 3(a)–3(d) for $d = 6, 4, 2.5,$ and 1.5 mm, respectively. We also utilize the analytical formula developed in [27] to theoretically estimate the number of longitudinal modes versus separation d with the interval of 0.5 mm, as depicted in Fig. 5, where the following parameters are employed: $h\nu_p = 2.46 \times 10^{-19}$ J, $\sigma_1 = 25 \times 10^{-19}$ cm², $\sigma_2 = 15.6 \times 10^{-19}$ cm², and $\tau_1 = \tau_2 = 100$ μ s, with other parameters as mentioned

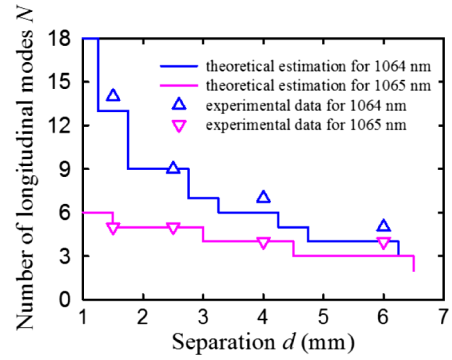


Fig. 5. Theoretical estimations and experimental data of picosecond Nd:YVO₄/Nd:LuVO₄ laser for the number of longitudinal modes with respect to the separation d .

before. The theoretical estimations can be found to be in excellent agreement with the experimental data, where the measured number of longitudinal modes for 1064 and 1065 nm are 5 and 4 for $d = 6$ mm, 7 and 4 for $d = 4$ mm, 9 and 5 for $d = 2.5$ mm, and 14 and 5 for $d = 1.5$ mm. Moreover, the total output powers for different separations d were experimentally found to be nearly invariant, as shown in Fig. 2(c). The corresponding autocorrelation traces for $d = 6, 4, 2.5,$ and 1.5 mm are shown in Figs. 4(a)–4(d), respectively. In addition, we numerically reconstruct the temporal behavior $E(t)$ of the dual-wavelength synchronous pulse by summing all fields of two groups of mode-locked states with the same angular frequency spacing $\Delta\omega$, that is

$$E(t) = \frac{1}{\sum_{i=1}^2 \beta_i} \left\{ \sum_{i=1}^2 \beta_i \left[\frac{1}{\sum_{s=0}^{N_i-1} A_{i,s}} \left(\sum_{s=0}^{N_i-1} A_{i,s} e^{i(\omega_{i,s}t + \phi_{i,s})} \right) \right] \right\}, \quad (1)$$

where β_i is the weighting factor for each spectral group; N_i is the number of longitudinal modes; $A_{i,s}$, $\omega_{i,s}$ ($= \omega_{i,0} + s \cdot \Delta\omega$), and $\phi_{i,s}$ are the amplitude, angular frequency, and phase for the s th lasing mode in each spectral group at λ_i , and $\omega_{i,0}$ could be deduced by the longest emission wavelength from optical spectra in Fig. 3. Under the assumption that all relative phase differences are zero, the normalized intensities of each 1064 and 1065 nm group together with their field summation for different separations d are simulated in the insets in Figs. 4(a)–4(d). It can be experimentally and numerically concluded that because the number of longitudinal modes increases with decreasing separation d , the pulse duration will monotonically reduce from 42 to 19 ps as the separation continuously varies from 6 to 1.5 mm. More intriguingly, the mismatch between the durations at 1064 and 1065 nm is found to lead the pulse behavior to gradually exhibit a particular shape featured by a broad wing part and a narrow central peak accompanied with the fully optically beat modulation. This behavior is more pronounced for the case of $d = 1.5$ mm.

Finally, it is worthwhile to mention that both the Nd:YVO₄ and Nd:LuVO₄ crystals belong to the narrow-band laser materials with fluorescent linewidths of less than 2 nm [30]. To further study the influence of the fluorescent bandwidth on our dual-wavelength mode-locked laser with respect to the SHB effect, the Nd:LuVO₄ crystal was replaced by a 5% Ng-cut Nd:KGW crystal with dimensions of 3 mm \times 3 mm \times 12 mm,

which is characterized by a much broader fluorescent bandwidth [31–33]. The optical spectra and the corresponding autocorrelation traces of the Nd:YVO₄/Nd:KGW laser for $d = 8, 6, 3,$ and 1 mm are illustrated in Figs. 6 and 7, respectively. The output powers for all cases are generally larger than 1.7 W under an incident pump power of 5.1 W, corresponding to an optical conversion efficiency higher than 33% . On the one hand, it can be seen that single pulse operation is achieved only when the SHB effect is greatly relieved, i.e., when the separation d is increased to a certain extent. Consequently, a somewhat wide pulse duration of 79 ps is obtained for $d = 8$ mm, in which a stream of subpicosecond optically beat pulses is produced with effective width as small as 0.6 ps and repetition rate as fast as 0.85 THz, as illustrated in Figs. 7(a) and 7(e). On the other hand, when the SHB effect is strengthened by decreasing the separation d , the spectral splitting, as shown in Figs. 6(b)–6(d), is experimentally

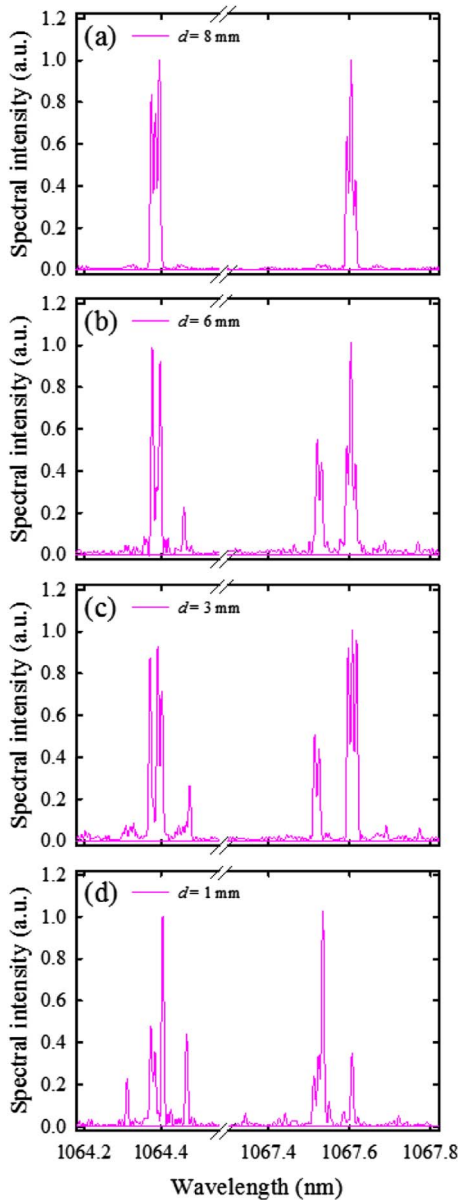


Fig. 6. Optical spectra of picosecond Nd:YVO₄/Nd:KGW laser for (a) $d = 8$ mm, (b) $d = 6$ mm, (c) $d = 3$ mm, and (d) $d = 1$ mm.

observed to cause the temporal behavior of the Nd:YVO₄/Nd:KGW picosecond laser to be in the multipulse state, as exhibited in Figs. 7(b)–7(d). We also utilize Eq. (1) to numerically reconstruct the temporal behaviors for each 1064 and 1067 nm group as well as their field summations for different separations d , where the normalized intensities are illustrated in the insets in Figs. 7(a)–7(d). The consistency between the

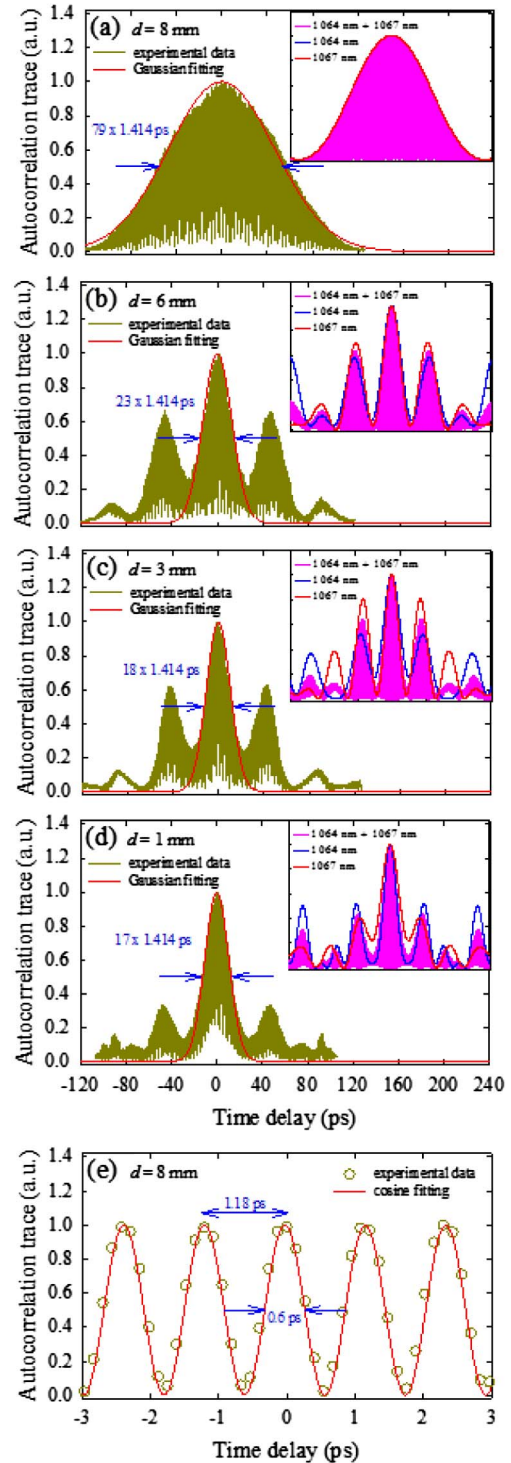


Fig. 7. Experimental autocorrelation traces and numerically reconstructed pulse shapes of picosecond Nd:YVO₄/Nd:KGW laser for (a) $d = 8$ mm, (b) $d = 6$ mm, (c) $d = 3$ mm, and (d) $d = 1$ mm. (e) Detailed structure of the optical beat pulse.

multipulse behavior and the spectral splitting can be found to nicely agree with the experimental observation. During the experiment, harmonic mode locking was not observed, and we utilize the relative frequency deviation of the fundamental harmonic $\Delta\nu/\nu$ to quantitatively characterize the stability of the dual-wavelength laser, where ν is the central frequency and $\Delta\nu$ is the FWHM of the fundamental harmonic, which can be determined by measuring the RF spectrum. For both the Nd:YVO₄/Nd:LuVO₄ and Nd:YVO₄/Nd:KGW schemes, the values are typically of the order of 10⁻⁴ with slightly larger value for smaller separation d due to the relatively strong mode competition as a result of the broader lasing spectral bandwidth. It is believed that the phenomena presented in this article can provide practical insights in designing a dual-wavelength synchronous picosecond laser based on the compactly combined dual gain media.

4. CONCLUSION

In summary, we have experimentally optimized the length of the Nd:YVO₄ crystal and combined it with the Nd:LuVO₄ or Nd:KGW crystals to successfully obtain a high-efficiency dual-wavelength self-mode-locked laser at 1.06 μm with the TEM₀₀ mode. We have further changed the separation between the input end mirror and the gain medium to explore the SHB effect on the mode-locked performance of the developed dual-wavelength picosecond laser. It has been experimentally and theoretically found that a shorter pulse duration can be accomplished with the smaller separation thanks to the wider emission spectrum via the enhancement of the SHB effect. In addition, the pulse behavior exhibits a narrow-peak-on-a-pedestal shape due to the appreciable mismatch between the pulse durations for the Nd:YVO₄/Nd:LuVO₄ scheme and would become a multipulse state due to the spectral splitting for the Nd:YVO₄/Nd:KGW configuration. Such concept of physically combining two gain media to generate dual-wavelength emission is also expected to be applicable for passive mode locking in the megahertz repetition rate regime with various kinds of saturable absorbers, from traditional SESAMs to newly developed nanotube, graphene, and few-layer MoS₂ [34–38] (especially featured by their broadband operation), which will be investigated in the future.

ACKNOWLEDGMENTS

The authors thank the National Science Council for financial support of this research under Contract No. NSC-100-2628-M-009-001-MY3.

REFERENCES

- B. M. Walsh, "Dual wavelength lasers," *Laser Phys.* **20**, 622–634 (2010).
- M. B. Danailov and I. Y. Milev, "Simultaneous multiwavelength operation of Nd:YAG laser," *Appl. Phys. Lett.* **61**, 746–748 (1992).
- B. Wu, P. Jiang, D. Yang, T. Chen, J. Kong, and Y. Shen, "Compact dual-wavelength Nd:GdVO₄ laser working at 1063 and 1065 nm," *Opt. Express* **17**, 6004–6009 (2009).
- P. Zhao, S. Ragam, Y. J. Ding, and I. B. Zotova, "Compact and portable terahertz source by mixing two frequencies generated simultaneously by a single solid-state laser," *Opt. Lett.* **35**, 3979–3981 (2010).
- A. A. Sirotkin, S. V. Garnov, V. I. Vlasov, A. I. Zagumennyi, Y. D. Zavartsev, S. A. Kutovoi, and I. A. Shcherbakov, "Two-frequency vanadate lasers with mutually parallel and orthogonal polarizations of radiation," *Quantum Electron.* **42**, 420–426 (2012).
- H. Yu, H. Zhang, Z. Wang, J. Wang, Y. Yu, Z. Shi, X. Zhang, and M. Liang, "High-power dual-wavelength laser with disordered Nd: CNGG crystals," *Opt. Lett.* **34**, 151–153 (2009).
- A. Brenier, Y. Wu, P. Fu, J. Zhang, and Y. Zu, "Diode-pumped laser properties of Nd³⁺-doped La₂CaB₁₀O₁₉ crystal including two-frequency generation with 4.6 THz separation," *Opt. Express* **17**, 18730–18737 (2009).
- G. Q. Xie, D. Y. Tang, H. Luo, H. J. Zhang, H. H. Yu, J. Y. Wang, X. T. Tao, M. H. Jiang, and L. J. Qian, "Dual-wavelength synchronously mode-locked Nd: CNGG laser," *Opt. Lett.* **33**, 1872–1874 (2008).
- A. Agnesi, F. Pirzio, G. Reali, A. Arcangeli, M. Tonelli, Z. Jia, and X. Tao, "Multi-wavelength diode-pumped Nd: LGGG picosecond laser," *Appl. Phys. B* **99**, 135–140 (2010).
- A. Agnesi, F. Pirzio, G. Reali, A. Arcangeli, M. Tonelli, Z. Jia, and X. Tao, "Multi-wavelength Nd: GAGG picosecond laser," *Opt. Mater.* **32**, 1130–1133 (2010).
- Z. Cong, D. Tang, W. D. Tan, J. Zhang, C. Xu, D. Luo, X. Xu, D. Li, J. Xu, X. Zhang, and Q. Wang, "Dual-wavelength passively mode-locked Nd: LuYSiO₅ laser with SESAM," *Opt. Express* **19**, 3984–3989 (2011).
- U. Keller, K. J. Weingarten, F. X. Kärtner, D. Kopf, B. Braun, I. D. Jung, R. Fluck, C. Hönninger, N. Matuschek, and J. Aus der Au, "Semiconductor saturable absorber mirrors (SESAMs) for femtosecond to nanosecond pulse generation in solid-state lasers," *IEEE J. Sel. Top. Quantum Electron.* **2**, 435–453 (1996).
- S. Tsuda, W. H. Knox, S. T. Cundiff, W. Y. Jan, and J. E. Cunningham, "Mode-locking ultrafast solid-state lasers with saturable Bragg reflectors," *IEEE J. Sel. Top. Quantum Electron.* **2**, 454–464 (1996).
- L. Krainer, R. Paschotta, J. Aus der Au, C. Hönninger, U. Keller, M. Moser, D. Kopf, and K. J. Weingarten, "Passively mode-locked Nd: YVO₄ laser with up to 13 GHz repetition rate," *Appl. Phys. B* **69**, 245–247 (1999).
- A. Agnesi, F. Pirzio, A. Tomaselli, G. Reali, and C. Braggio, "Multi-GHz tunable-repetition-rate mode-locked Nd: GdVO₄ laser," *Opt. Express* **13**, 5302–5307 (2005).
- A. E. H. Oehler, T. Südmeier, K. J. Weingarten, and U. Keller, "100 GHz passively mode-locked Er: Yb: glass laser at 1.5 μm with 1.6-ps pulses," *Opt. Express* **16**, 21930–21935 (2008).
- H. C. Liang, R. C. C. Chen, Y. J. Huang, K. W. Su, and Y. F. Chen, "Compact efficient multi-GHz Kerr-lens mode-locked diode-pumped Nd: YVO₄ laser," *Opt. Express* **16**, 21149–21154 (2008).
- H. C. Liang, Y. J. Huang, W. C. Huang, K. W. Su, and Y. F. Chen, "High-power, diode-end-pumped, multigigahertz self-mode-locked Nd: YVO₄ laser at 1342 nm," *Opt. Lett.* **35**, 4–6 (2010).
- Y. J. Huang, Y. S. Tzeng, C. Y. Tang, Y. P. Huang, and Y. F. Chen, "Tunable GHz pulse repetition rate operation in high-power TEM₀₀-mode Nd: YLF lasers at 1047 nm and 1053 nm with self mode locking," *Opt. Express* **20**, 18230–18237 (2012).
- L. Kornaszewski, G. Maker, G. P. A. Malcolm, M. Butkus, E. U. Rafailov, and C. J. Hamilton, "SESAM-free mode-locked semiconductor disk laser," *Laser Photon. Rev.* **6**, L20–L23 (2012).
- M. Gaafar, D. A. Nakdali, C. Möller, K. A. Fedorova, M. Wichmann, M. K. Shakfa, F. Zhang, A. Rahimi-Iman, E. U. Rafailov, and M. Koch, "Self-mode-locked quantum-dot vertical-external-cavity surface-emitting laser," *Opt. Lett.* **39**, 4623–4626 (2014).
- Y. J. Huang, Y. S. Tzeng, C. Y. Tang, S. Y. Chiang, H. C. Liang, and Y. F. Chen, "Efficient high-power terahertz beating in a dual-wavelength synchronously mode-locked laser with dual gain media," *Opt. Lett.* **39**, 1477–1480 (2014).
- C. J. Flood, D. R. Walker, and H. M. van Driel, "Effect of spatial hole burning in a mode-locked diode end-pumped Nd: YAG laser," *Opt. Lett.* **20**, 58–60 (1995).
- B. Braun, K. J. Weingarten, F. X. Kärtner, and U. Keller, "Continuous-wave mode-locked solid-state lasers with enhanced spatial hole burning," *Appl. Phys. B* **61**, 429–437 (1995).
- Y. J. Huang, Y. P. Huang, H. C. Liang, K. W. Su, Y. F. Chen, and K. F. Huang, "Comparative study between conventional and diffusion-bonded Nd-doped vanadate crystals in the passively mode-locked operation," *Opt. Express* **18**, 9518–9524 (2010).

26. C. Schäfer, C. Theobald, R. Wallenstein, and J. A. L'huillier, "Effects of spatial hole burning in 888 nm pumped, passively mode-locked high-power Nd:YVO₄ lasers," *Appl. Phys. B* **102**, 523–528 (2011).
27. Y. F. Chen, Y. J. Huang, P. Y. Chiang, Y. C. Lin, and H. C. Liang, "Controlling number of lasing modes for designing short-cavity self-mode-locked Nd-doped vanadate lasers," *Appl. Phys. B* **103**, 841–846 (2011).
28. Y. J. Huang, Y. S. Tzeng, C. Y. Tang, and Y. F. Chen, "Efficient dual-wavelength synchronously mode-locked picosecond laser operating on the $^4F_{3/2} \rightarrow ^4I_{11/2}$ transition with compactly combined dual gain media," *IEEE J. Sel. Top. Quantum Electron.* **21**, 1100107 (2015).
29. X. Liu, D. Han, Z. Sun, C. Zeng, H. Lu, D. Mao, Y. Cui, and F. Wang, "Versatile multi-wavelength ultrafast fiber laser mode-locked by carbon nanotubes," *Sci. Rep.* **3**, 2718 (2013).
30. H. H. Yu, H. J. Zhang, D. Y. Tang, Z. P. Wang, J. Y. Wang, Y. G. Yu, G. Q. Xie, H. Luo, and M. H. Jiang, "Diode-end-pumped passively mode-locked Nd:LuVO₄ laser with a semiconductor saturable-absorber mirror," *Appl. Phys. B* **91**, 425–428 (2008).
31. C. J. Flood, D. R. Walker, and H. M. van Driel, "CW diode pumping and FM mode locking of a Nd:KGW laser," *Appl. Phys. B* **60**, 309–312 (1995).
32. Y. Chen, L. Major, and V. Kushawaha, "Efficient laser operation of diode-pumped Nd:KGd(WO₄)₂ crystal at 1.067 μm ," *Appl. Opt.* **35**, 3203–3206 (1996).
33. A. Major, N. Langford, T. Graf, D. Burns, and A. I. Ferguson, "Diode-pumped passively mode-locked Nd:KGd(WO₄)₂ laser with 1-W average output power," *Opt. Lett.* **27**, 1478–1480 (2002).
34. W. D. Tan, C. Y. Su, R. J. Knize, G. Q. Xie, L. J. Li, and D. Y. Tang, "Mode locking of ceramic Nd:yttrium aluminum garnet with graphene as a saturable absorber," *Appl. Phys. Lett.* **96**, 031106 (2010).
35. A. Agnesi, A. Greborio, F. Pirzio, G. Reali, S. Y. Choi, F. Rotermund, U. Griebner, and V. Petrov, "99 fs Nd:glass laser mode-locked with carbon nanotube saturable absorber mirror," *Appl. Phys. Express* **3**, 112702 (2010).
36. Z. Sun, T. Hasan, and A. C. Ferrari, "Ultrafast lasers mode-locked by nanotubes and graphene," *Physica E* **44**, 1082–1091 (2012).
37. A. Martinez and Z. Sun, "Nanotube and graphene saturable absorbers for fibre lasers," *Nat. Photonics* **7**, 842–845 (2013).
38. H. Zhang, S. B. Lu, J. Zheng, J. Du, S. C. Wen, D. Y. Tang, and K. P. Loh, "Molybdenum disulfide (MoS₂) as a broadband saturable absorber for ultra-fast photonics," *Opt. Express* **22**, 7249–7260 (2014).